Validation and Application of a Code for 3-D Analysis of Hydrogen Behavior during Severe Accidents

Jongtae Kim [a*], Hyoung Tae Kim [a], Dehee Kim [a]
[a] *KAERI, Daeduk-daero 989-111, Daejeon, Korea*
[*] *Corresponding author: ex-kjt@kaeri.re.kr*

1. Introduction

During a loss of coolant accident (LOCA) or a station blackout accident (SBO) in a pressurized water reactor, hot water and steam is released into the containment building. The water vapor released into the containment mixes with the atmosphere and partially condenses into droplets or condenses on the surface of the structure in the containment building, raising the temperature of the structure and running down the walls as liquid films or drops. However, a large amount of water vapor is not condensed and remains in the containment building.

When hydrogen generated by core oxidation is released into the containment, it diffuses as it mixes with the water vapor and the atmosphere, which is the non-condensable gas in the containment. As the concentration of water vapor increases in any space in the containment, the concentration of hydrogen will be relatively lowered, and the potential for explosion or flame acceleration will be reduced. Hydrogen concentrations below 4 vol% are known to be non-flammable, meaning that combustion does not occur. Also, as the concentration of water vapor increases and reaches 65 vol% or more, combustion becomes unlikely even if the concentration of hydrogen is high.

Thus, the behavior of water vapor in a containment building directly affects the distribution of hydrogen. As the water vapor changes phase with saturation in the containment and becomes liquid water, it no longer contributes to the concentration of hydrogen, but it can indirectly affect the behavior of hydrogen through thermal and flow resistance.

Recently a turbulence-resolved CFD (computation fluid dynamics) code, contain3D, has been developed for a hydrogen safety analysis in an NPP containment for best estimation [1, 2].

This paper introduces the analytical models implemented in the code and its validation results. The code was applied to study hydrogen behaviors affected by water vapor condensation and hydrogen recombination by PARs installed in the APR1400 containment, and the results were discussed in this study.

2. Modeling

Volumetric condensation is the condensation of supersaturated water vapor when the atmosphere contains more water vapor than the saturated water vapor pressure corresponding to its temperature and is an important factor that directly affects the distribution and concentration of hydrogen in an actual containment building.

2.1 Governing Equations

Equations (1) through (4) represent the governing equations for the gas phase assuming thermal and mechanical equilibrium with the fog phase.

$$\frac{\partial \rho}{\partial t} + \nabla \cdot (\rho \boldsymbol{U}) = S_\rho \tag{1}$$

$$\frac{\partial}{\partial t}(\rho \boldsymbol{U}) + \nabla \cdot (\rho \boldsymbol{U}\boldsymbol{U}) - \nabla \cdot \boldsymbol{R} = -\nabla \mathrm{p} + \rho \boldsymbol{g} + \boldsymbol{S}_m \tag{2}$$

$$\frac{\partial}{\partial t}(\rho Y_i) + \nabla \cdot (\rho Y_i \boldsymbol{U}) - \nabla \cdot \boldsymbol{J}_i = S_{Y_i} \tag{3}$$

$$\frac{\partial}{\partial t}(\rho h_s) + \nabla \cdot (\rho h_s \boldsymbol{U}) - \nabla \cdot \boldsymbol{q} = \frac{\partial p}{\partial t} - \left[\frac{\partial}{\partial t}(\rho K) + \nabla \cdot (\rho K \boldsymbol{U})\right] + S_h \tag{4}$$

The mass faction of the fog phase is defined as a ratio of fog mass to gas mass instead of the total mass of fog and gas.

$$\boldsymbol{\alpha} = \frac{m_f}{m_g} \tag{5}$$

Eq. (6) is the fog mass transport equation, and the rate of water vapor condensation and fog evaporation, S_α, is simply modeled by Eq. (7).

$$\frac{\partial}{\partial t}(\rho_g \alpha) + \nabla(\rho_g \boldsymbol{U} \alpha) - \nabla(\Gamma_t \nabla \alpha) = S_\alpha \tag{6}$$

$$S_\alpha = C_{blk}(\rho_{sat} - \rho_{h2o}) \tag{7}$$

2.2 Modeling for gas species diffusion

When water vapor released into a containment building mixes with the atmosphere and condenses on the walls, the condensation rate is limited by diffusion rate. So it is called a diffusion-controlled condensation. Therefore, a diffusion model for gas species is required to simulate condensation of water vapor mixed with air and hydrogen in a containment building.

The diffusive flux of a gas species is governed by the Fick law and is expressed as a function of the concentration gradient of a gas species *i* and the mass diffusivity. Eq. (8) represents the total mass diffusion, including molecular diffusion and turbulent diffusion.

$$\boldsymbol{J}_i = \rho D_{im} \nabla Y_i - \rho Y_i V_c + \frac{\rho \nu_t}{Sc_t} \nabla Y_i \tag{8}$$

The first term on the right-hand side of Eq. (8) is the molecular diffusion flux and the second term is a correction flux to satisfy the sum of the species diffusion fluxes to zero. The last term is a turbulent diffusion flux due to the Boussinesq assumption.

Fig. 1 shows the list of diffusion coefficient models included in the developed diffusion model. There are currently four diffusion coefficient models in use, increasing in complexity and computation from bottom to top. The simplest diffusion coefficient model is the constant Schmidt diffusion coefficient (constSchmidt-DiffusionCoefficient) model, which uses a constant diffusion coefficient for all species based on the number of $Sc(=\nu_i/D_{im})$ entered by the user.

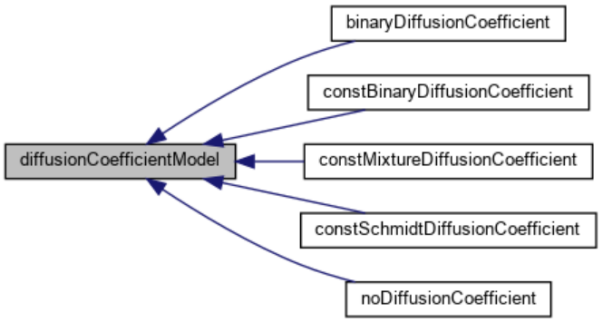

Fig. 1. Gas diffusion model hierarchy

2.3 Modeling for wall condensation and heat transfer

In general wall heat transfer can be considered by a conjugate heat transfer (CHT) approach, which needs a solid heat conduction solver coupled with a fluid solver. In addition to the CHT multi-region 1-dimensional heat conduction model is implemented in the contain3d code for a fast simulation of containment thermal-hydraulics. It solves the 1-D unsteady heat conduction equation coupled with fluid boundary.

The wall condensation rate or condensation mass flow rate of water vapor is expressed by the rate of diffusion through non-condensable gases as shown in Eq. (9).

$$\dot{m}'' = \rho \frac{D_w}{\delta} \frac{(Y_{h2o,i} - Y_{h2o,w})}{(1 - Y_{h2o,w})} \tag{9}$$

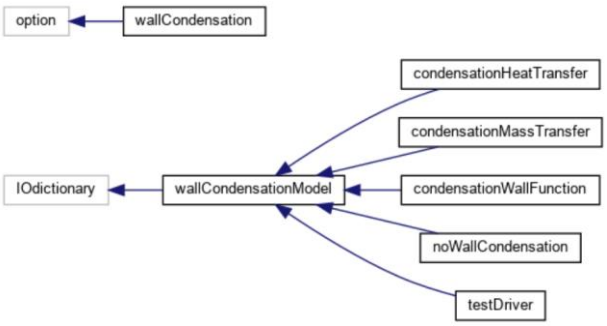

Fig. 2. Condensation model hierarchy.

Fig. 2 shows the hierarchy of the condensation models. The CondensationHeatTransfer class is based on the heat transfer correlation for water vapor condensation, condensationMassTransfer is a model based on the mass diffusion correlation, and condensationWallFunction is a condensation model based on a wall function.

Wall condensation of water vapor depends on the wall temperature, i.e., the wall water vapor condensation rate is a function of the wall temperature. The currently developed wall condensation analysis module is associated with three different wall temperature boundary conditions (shown in Fig. 3), which are constant wall temperature, 1-D, and 3-D heat conduction boundary conditions.

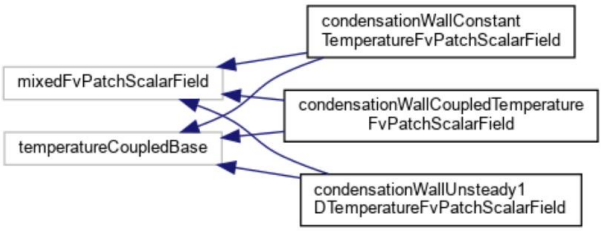

Fig. 3. Hierarchy of wall heat transfer models coupled with wall condensation.

2.4 Modeling for PARs

PAR consists of a catalyst and a duct (or chamber), and the catalyst is made in various forms depending on the manufacturer. The duct of the PAR separates the hot exhaust gas generated by the catalytic reaction from the PAR external and creates buoyancy due to the density difference between the inside and outside, which causes natural convection flow from the bottom to the top of the duct. The hydrogen mixture gas introduced into the duct entrance passes through the catalyst, and hydrogen and oxygen react to produce water vapor by catalytic reaction. The hydrogen catalytic reaction is exothermic and generates heat, part of which is absorbed by the catalyst and part by the exhaust gas. The generated energy in Eq. (10) is based on the mass of hydrogen reacted.

$$\mathrm{H}_2 + \frac{1}{2}O_2 \Rightarrow H_2O + 122\ [MJ/kg] \tag{10}$$

The reaction rate of Eq. (10) by a PAR is called hydrogen recombination or removal rate, which is normally provided by the manufacturer.

The hydrogen removal rate of a PAR is affected by the gas mass flow rate at the duct inlet, and the diffusion rate of hydrogen to the catalyst surface.

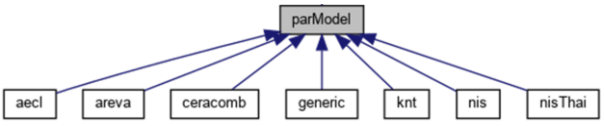

Fig. 4. PAR model hierarchy.

Fig. 4 shows the configuration of the PAR analysis module, which contains 7 par models.

3. Validation Results

The TOSQAN project [4] was conducted to experimentally simulate the thermal-hydraulic flow behavior in an accident and to study wall condensation phenomenon in the presence of non-condensable gases. Fig 5. shows the test vessel with a height of 4.8 m, a diameter of 1.5 m, and a gas volume of 7 m^3. And Fig. 6.

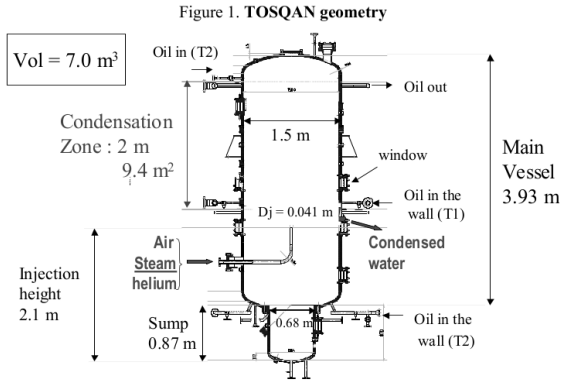

Fig. 5. TOSQAN test facility

The experiment was conducted in multiple phases, each of which varied the injection conditions of water vapor, air, and helium. Fig. 10 shows the injection flow rates of the gas species in the TOSQAN ISP-47 test.

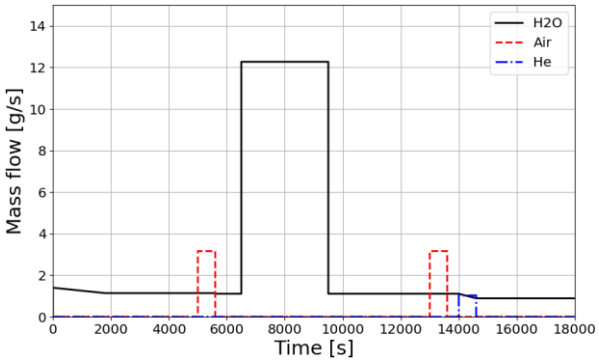

Fig. 6. TOSQAN ISP-47 test conditions.

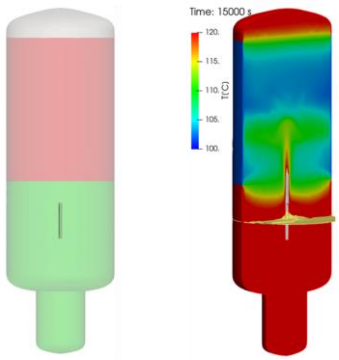

Fig. 7. TOSQAN wall patches and temperature distribution by the simulation.

The TOSQAN ISP-47 test was simulated to validate the turbulent diffusion and condensation models implemented in the 3-D code. The geometry and the vessel wall patches used in the simulation are shown in Fig. 7.

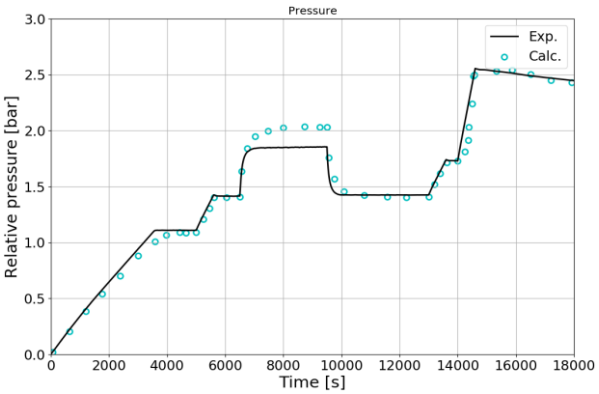

Fig. 8. Comparison of pressure change over time.

Fig. 7 and 8 are the results of the simulation using the 3-D code. Because of the condensing wall in upper part of the vessel temperature distribution was strongly affected. The pressure change by the gas injections and wall condensation are well predicted compared with the experimental results.

Verification calculation of the PAR analysis module were performed using the THAI HR-17 test results. The HR-17 experiment is an experiment using a 0.52 scale device of AECL PAR, and the initial conditions are a pressure of 1.5 bar, a temperature of 25 ℃, and a dry air experiment without water vapor injection.

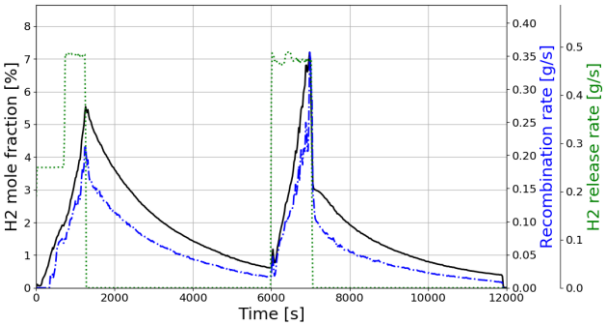

Fig. 9. Hydrogen injection rate, PAR inlet hydrogen concentration, and PAR recombination rate in HR-17 test.

Fig. 9 shows the hydrogen release rate, PAR inlet hydrogen concentration, and recombination rate of PAR over time in the HR-17 experiment. A spontaneous ignition occurred at about 7040 seconds in the second stage hydrogen injection. As shown in the figure, the initial operation of the PAR starts at about 340 seconds after the start of hydrogen injection.

Fig. 10 compares the hydrogen recombination rate of the PAR from the experimental data and the calculation result of the PAR analysis module over time. It is thought that the currently developed PAR analysis module predicts the characteristics of the PAR recombination well.

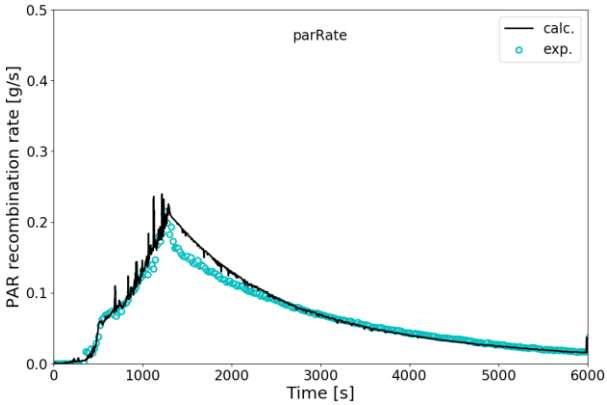

Fig. 10. Comparison of PAR recombination rate in the HR-17 test.

4. Application Results

Severe accident scenario chosen in this study for a hydrogen behavior analysis is a SBLOCA in APR1400. Accident progression of APR1400 was calculated by the MELCOR code [5].

In the case of the APR1400 nuclear reactor, the total amount of hydrogen generated by 100% oxidation of the active core is approximately 1000 kg. It is still considered so much conservative that the active core is fully oxidized until the reactor vessel is failed. But because the current oxidation model used in the MELCOR code is not validated to be applicable to a debris formed on the core support plate or the lower plenum of the vessel, it is persuasive to consider 100 % oxidation of the active core as a conservative point of view.

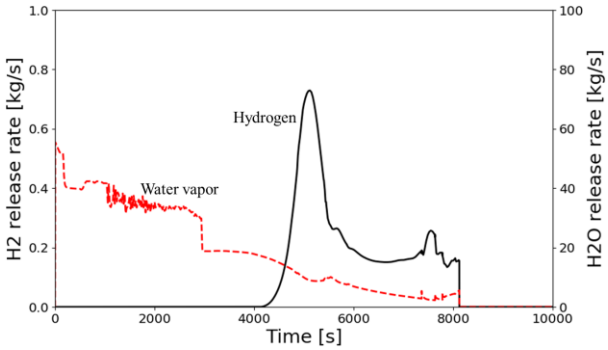

Fig. 11. Water vapor and hydrogen release rates in the case of the APR1400 SBLOCA accident.

In the early stage of a SBLOCA accident, water vapor release rate is high due to high reactor pressure, and release rate decreases as the accident progresses (Fig. 11). Fig. 12 shows the distribution of water vapor in the containment building over time. 5000 seconds after start of the accident, the water vapor concentration in the containment increases to 70%. It can then be seen that as the water vapor release rate decreases, its concentration in the containment decreases due to vapor condensation.

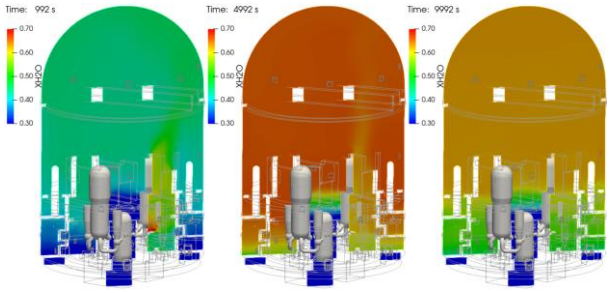

Fig. 12. Change of water vapor distribution during the SBLOCA in the APR1400 containment.

Fig. 13 shows the evolution of hydrogen distribution in the containment over time, with hydrogen being well mixed by the strong upward flow of the released water vapor. In the figure at 9992 seconds, the hydrogen concentration is higher in the lower part of the containment, which is strongly related to the water vapor distribution.

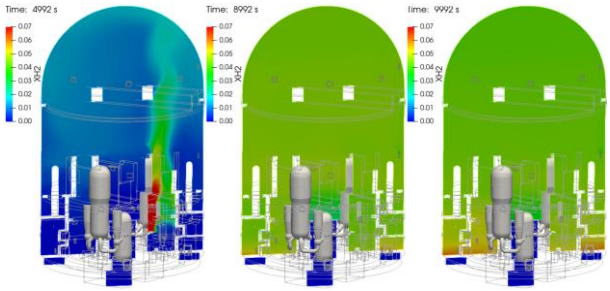

Fig. 13. Change of hydrogen distribution during the SBLOCA in the APR1400 containment.

4. Conclusions

In this study, a three-dimensional analysis code for hydrogen distribution in containment buildings was verified and applied to a real nuclear power plant. During a severe accident, huge amount of water vapor is released into the containment, and its thermal hydraulic behaviors directly affects the distribution of the hydrogen released with the steam. The results from the APR1400 accident analyses clearly show the interaction between the behaviors of water vapor and hydrogen.

ACKNOWLEDGMENTS

This work was supported by the Korea Foundation of Nuclear Safety (KOFONS) (No. 2106007).

REFERENCES

[1] J. Kim, J. Jung, and D. Kim, “Methodology Development for Evaluation of Hydrogen Safety in a NPP Containment Using OpenFOAM”, Technical Meeting on Hydrogen Management in Severe Accidents, IAEA, 2018.
[2] J. Kim, et al., Establishment of a base system for 3D analysis of hydrogen distribution in a containment building, KINS Contract Report, 2021
[3] V.V. Toro, A.V. Mokhov, H.B. Levinsky, M.D. Smooke, “Combined experimental and computational study of laminar

hydrogen-air diffusion flames," Proc. Combust, Inst. 30, 2005, pp. 485-492.
[4] J. Malet, E. Porcheron, F. Dumay, J. Vendel, "Code-experiment comparison on wall condensation tests in the presence of non-condensable gases—Numerical calculations for containment studies", Nuclear Engineering and Design 253 (2012) 98–113
[5] L.L. Humphries, B.A. Beeny, F. Gelbard, D.L. Louie, J. Phillips, "MELCOR Computer Code Manuals Vol. 1: Primer and Users' Guide Version 2.2", USNRC, 2017